

Dissolution Phenomenon of the Piretanide Amorphous Form Involving Phase Change

Yuji CHIKARAISHI,*^a Makoto OTSUKA,^b and Yoshihisa MATSUDA^b

Nippon Hoechst Marion Roussel Ltd., Research and Development Division, Preclinical Development Laboratories,^a Minamidai, Kawagoe, Saitama 350–11, Japan and Kobe Pharmaceutical University,^b Motoyama-Kitamachi, Higashi-Nada, Kobe 658, Japan. Received April 26, 1996; accepted July 23, 1996

The dissolution phenomenon of piretanide amorphous form and form C was investigated in various pH buffers at 37°C and at pH 5 at various temperatures by a dispersed-amount method. Their initial dissolution rates were investigated at pH 5 at various temperatures (30–45°C) by a stationary-disk method. The solubility of the amorphous form and form C was temperature dependent at pH 5 and pH dependent at 37°C. The amorphous form was more soluble than form C under acidic conditions. However, it was as soluble as form C in JP XII second fluid (pH 6.8). The amorphous form showed characteristic convex dissolution curves with maximal concentration at 30 and 35°C, whereas the amorphous form at 40 and 45°C and the form C at 30–45°C showed only normal dissolution curves. The initial dissolution process of form C obtained by the stationary-disk method followed the Noyes–Whitney–Nernst equation, but that of the amorphous form did not. The initial dissolution process of the amorphous form was analyzed by a dissolution kinetics equation involving phase transformation from the amorphous form to form C. The maximal concentration, the dissolution rate constant, and the rate constant of the phase transition process were estimated. The thermodynamic parameters for the dissolution process of the amorphous form and form C were obtained from van't Hoff and Arrhenius plots, respectively. The results of the intrinsic solubility and dissolution parameters of the two forms suggested that the difference in the dissolution rates between them affects the bioavailability of piretanide preparations.

Key words piretanide; amorphous form; solubility; initial dissolution rate; stationary disk method

Solubility and dissolution rate are two of the most important factors affecting bioavailability. In general, many organic compounds showed normal dissolution curves when examined by the dispersed-amount method and the initial dissolution process followed the Noyes–Whitney–Nernst equation. We reported that the forms A and B of piretanide (3-(aminosulfonyl)-4-phenoxy-5-(1-pyrrolidinyl)benzoic acid; IUPAC) (Fig. 1) showed the normal dissolution curves and that the initial dissolution process followed the Noyes–Whitney–Nernst equation.¹⁾ However, characteristic convex dissolution curves at maximal concentration have been observed during the dissolution of polymorphs.^{2–8)}

In this present study, we investigated the effect of temperature and pH on the dissolution behavior of the amorphous form and form C. The amorphous form showed characteristic dissolution behavior in this study, so it was difficult to estimate its intrinsic solubility because it transformed into form C before the concentration of the dissolved drug reached equilibrium solubility. Therefore, the dissolution behavior and solubility of the amorphous form and form C at pH 5 were evaluated using a stationary-disk method based on the dissolution kinetic model.

Experimental

Materials A piretanide bulk sample (lot No. L023, L024) was obtained from Hoechst Aktiengesellschaft, Germany. The amorphous form and form C were prepared as reported.⁹⁾ The pellets for the stationary-disk method were prepared as follows: a 200 mg sample of powder was compressed in a cylindrical die of 13-mm diameter at about 1000 kg/cm² using an accurate compression/tension testing machine, then the compressed pellet was maintained for 1 min in the die at that pressure. The ejected pellet was fixed to a dissolution ring holder with beeswax so that only one side of the pellet surface was exposed.

X-Ray Powder Diffraction Analysis X-Ray powder diffraction pro-

files were taken at room temperature with an X-ray powder diffractometer (MXP³, Mac Science Co.). The operating conditions were as follows: target, Cu; filter, Ni; voltage, 30 kV; current, 10 mA; receiving slit, 0.15 mm; scanning speed 5° 2θ/min.

Dissolution Study Using the Dispersed-Amount Method Various pH dissolution media were obtained as follows: JP XII, first fluid (pH 1.2): 2.0 g of NaCl was added to 7.0 ml of HCl and the mixture was diluted with water to 1000 ml. JP XII, second fluid (pH 6.8): 118 ml of 0.2 N NaOH was added to 250 ml of 0.2 M KH₂PO₄ and the mixture was diluted with water to 1000 ml. pH 1 buffer, KCl–HCl¹⁰⁾: 407 ml of 0.2 M HCl and 93 ml of 0.2 M KCl made up to 1000 ml. pH 3 buffer, NaCl–glycine–HCl¹¹⁾: 32 ml of 2.5 M NaCl, 31.6 ml of 0.5 M glycine–0.5 M NaCl and 21.0 ml of 0.2 M HCl made up to 1000 ml. pH 5 buffer, NaCl–CH₃COONa–CH₃COOH¹¹⁾: 32 ml of 2.5 M NaCl, 20.0 ml of 1.0 M sodium acetate and 40.0 ml of 0.35 M acetic acid made up to 1000 ml. pH 6 buffer, NaCl–NaH₂PO₄–Na₂HPO₄¹¹⁾: 16 ml of 5 M NaCl, 3.3 ml of 4.0 M NaH₂PO₄ and 4.6 ml of 0.5 M Na₂HPO₄ made up to 1000 ml.

The dissolution profiles of the amorphous form and form C were investigated in the above solutions. An excess (500 mg) of sample was introduced into 250 ml of dissolution medium in a 1000-ml round-bottomed flask with a plastic cover. The flask was fixed on a sample holder in a thermostatically regulated water bath maintained at 37 ± 0.5 °C, and stirred by a paddle at 200 rpm. Aliquots (10 ml) of the solution were withdrawn at various intervals with a syringe through a 0.45-μm membrane. The filtrate was diluted and the concentration of the drug was measured at 275 nm using a spectrophotometer (type 430B, Jasco Co.). The dissolution profiles of the amorphous form and form C were

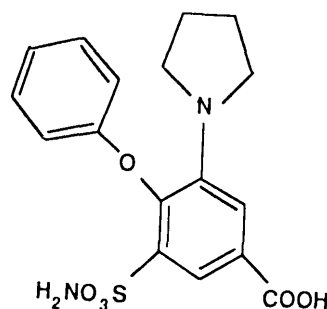


Fig. 1. Structure of Piretanide

* To whom correspondence should be addressed.

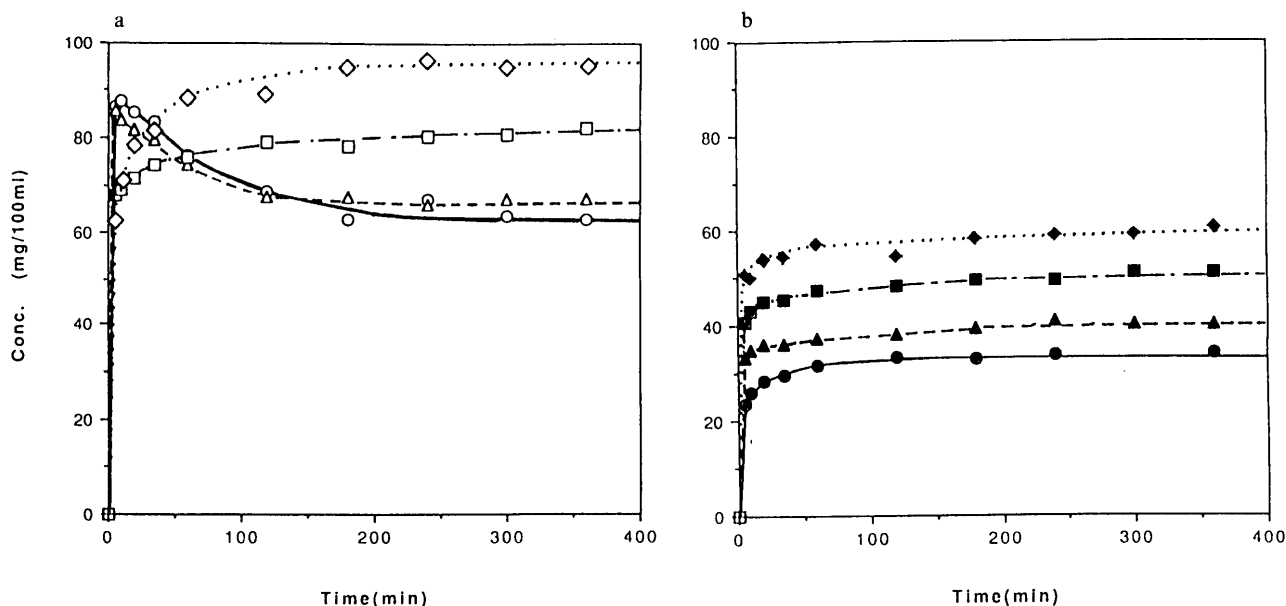


Fig. 2. Solubilities of Piretanide Amorphous Form (Open Symbols) and Form C (Closed Symbols) at Various Temperatures at pH 5

(a) ○, 30 °C; △, 35 °C; □, 40 °C; ◇, 45 °C. (b) ●, 30 °C; ▲, 35 °C; ■, 40 °C; ◆, 45 °C.

also investigated in pH 5 buffer at various dissolution medium temperatures (30–45 °C). The procedure was as described above.

Initial Dissolution Curve Measurement The initial dissolution profiles of the amorphous form and form C were investigated after the pellet was fixed on the dissolution ring holder under the conditions described above, except that 200 ml of dissolution medium was used, and the solution was introduced into a quartz flow-through cell with a peristaltic pump.

Kinetic Interpretation of the Transformation of the Amorphous Form to Form C during the Dissolution Process The initial dissolution curves of the amorphous form and form C were determined as described above. The computer program MULTI¹² performed the nonlinear least-squares analysis of the dissolution kinetics equation. The kinetic parameters were calculated by means of the damping Gauss–Newton method, after the initial values of the parameters were determined by the Simplex method. The weight of unity was used in this analysis.

Results and Discussion

Dissolution Profiles of Amorphous Form and Form C Obtained by the Dispersed-Amount Method Figure 2 (a and b) shows the dissolution profiles of the amorphous form and form C obtained by the dispersed-amount method at pH 5 at various temperatures. The concentration of the amorphous form reached a maximum more quickly than that of form C, then decreased gradually at 30 and 35 °C. The amorphous form showed characteristic convex dissolution curves with maximal solubility at 30 and 35 °C. In spite of the amorphous form at 40 and 45 °C and form C at 30–45 °C, normal dissolution curves had no maximum value. The crystallization process of amorphous form with a phase change to form C at 40 and 45 °C was faster than that at 30 and 35 °C. The dissolution curves of the amorphous form by the dispersed-amount method at 30 and 35 °C were similar to those of chlorpropamide,² theophylline,³ predonisolone,⁴ phenobarbital and *p*-hydroxybenzoic acid,⁵ phenylbutazone,⁶ and nitrofurantoin^{7,8} involving a crystallization process together with a phase change from the amorphous form to form C. Furthermore, the solubility of the amorphous form and form C depended on the temperature at pH 5.

Figure 3 shows that the solubilities of the amorphous

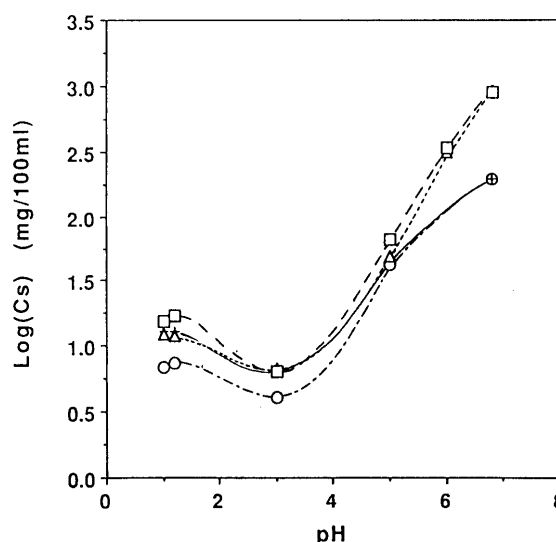


Fig. 3. Effect of pH on the Solubility of Piretanide Polymorphs at 37 °C

○, form A; +, form B; △, form C; □, amorphous form.

form and form C depended on the pH of the buffer. Forms A and B are shown for reference. After the dissolution of form C, the X-ray powder diffraction patterns of the crystallized precipitate coincided with that of the intact form. However, the amorphous form was changed to form C at various pH.

X-Ray Powder Diffraction Analysis of Amorphous Form and Form C The amorphous form exhibited no diffraction peak, but instead displayed a halo, while form C had nine main diffraction peaks at 10.5, 12.2, 15.6, 19.1, 19.9, 22.0, 22.8, 25.6 and 30.6° (2θ), indicating that both modifications produce significantly different diffraction profiles as reported.⁹ After the dissolution studies described above, X-ray powder diffraction profiles of the crystallized precipitates in various solutions coincided with that of intact form C (Fig. 4). That is to say, a

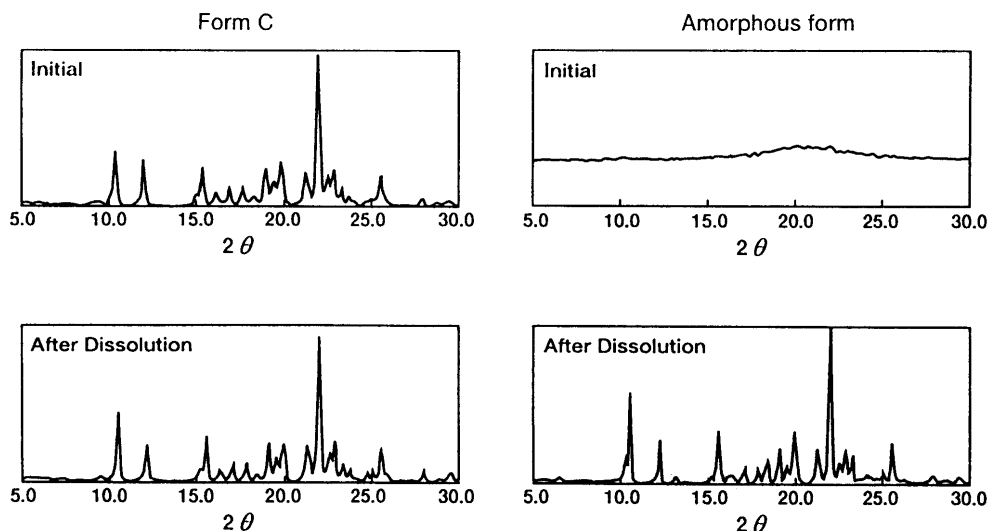


Fig. 4. X-Ray Powder Diffraction Profiles of Piretanide Amorphous Form and Form C before and after Dissolution

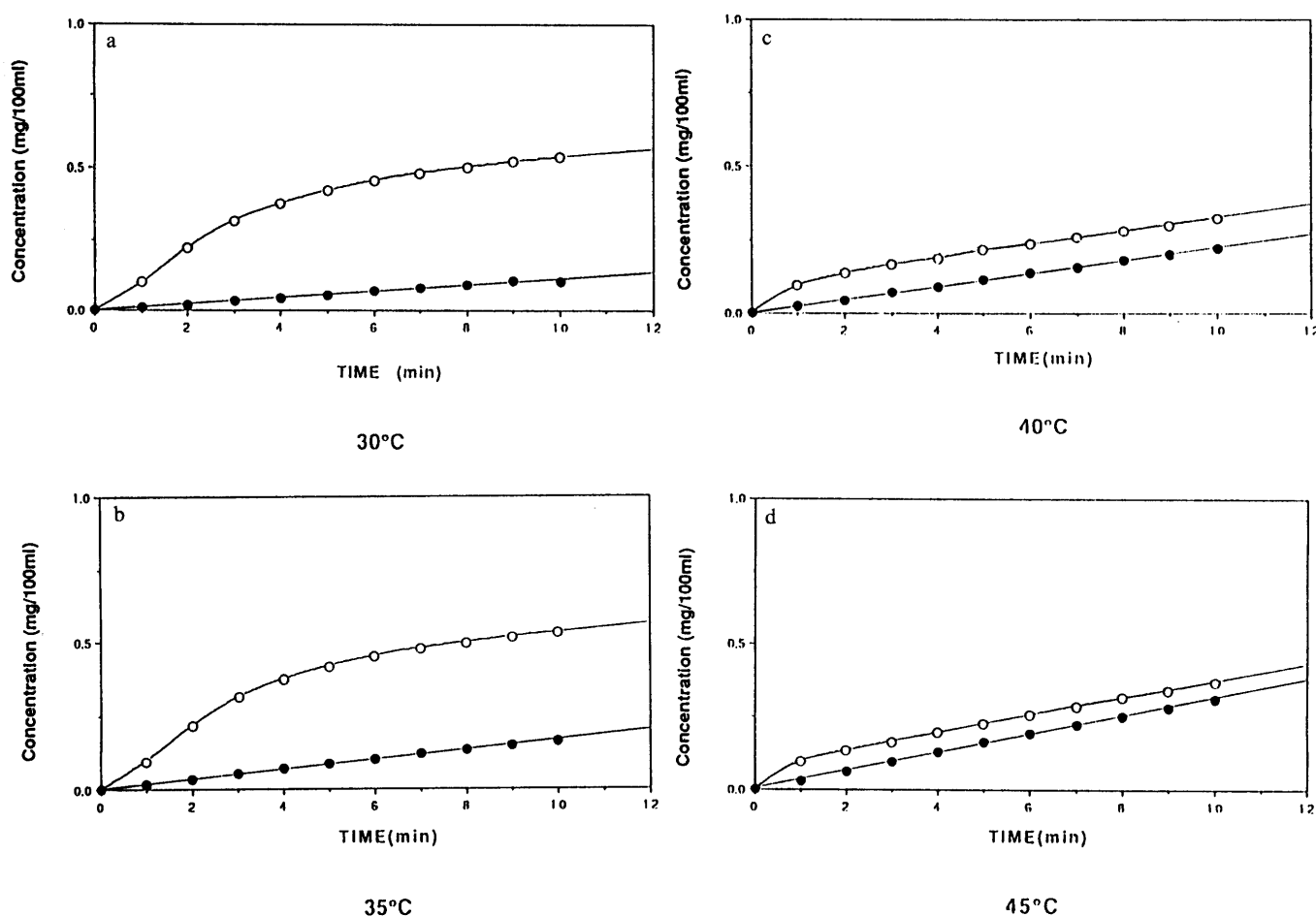


Fig. 5. Initial Dissolution Rate of Piretanide Amorphous Form (Open Symbols) and Form C (Closed Symbols) at Various Temperatures at pH 5 (a) 30°C, (b) 35°C, (c) 40°C, (d) 45°C.

crystallographic change occurred in the amorphous form during the dissolution test under our experimental conditions. Moreover, after compression at about 1000 kg/cm², the pellets of the amorphous form and form C were ground with an agate mortar and pestle, then the X-ray powder diffraction profiles were recorded. The profiles of all crystal forms of the compressed amorphous form and form C were identical to those of the original

samples. The X-ray diffraction profiles suggested these crystal forms did not undergo any crystallographic changes during the compression process under our experimental conditions.

Dissolution Profiles of Amorphous Form and Form C Obtained by the Stationary-Disk Method Figure 5 (a, b, c and d) shows the initial dissolution curves of the amorphous form and form C at pH 5 at 30–45°C by the

Table 1. Comparison of the Initial Dissolution Rate of Piretanide between Amorphous Forms and Form C at Various Temperatures at pH 5 after the Curve in the Initial Stage

Temperature (°C)	Initial dissolution rate (μg/ml/min)	
	Form C	Amorphous form
30	0.111	0.106
35	0.168	0.178
40	0.224	0.226
45	0.313	0.298

$n=3$.

stationary-disk method. A straight line was obtained for form C, and the line was estimated to be in sink conditions within 0–10 min. However, the initial dissolution curves of the amorphous form showed a straight line after the curve at an early stage. That is, the dissolution process of form C followed the Noyes–Whitney–Nernst equation, whereas that of the amorphous form did not. The slope of the dissolution curve of the amorphous form after the completion of the transformation accompanying crystallization was similar to that of form C. Furthermore, the initial dissolution rate of the amorphous form after the curve in the initial stage was coincident with that of form C at various temperatures as shown in Table 1. These values increased more or less with elevation of temperature.

Nogami *et al.*⁵⁾ reported the dissolution phenomena of *p*-hydroxybenzoic acid and phenobarbital, involving a simultaneous phase change from anhydrate to hydrate. They considered the diffusion constant of the anhydrate to be similar to that of the hydrate and proposed the following equation for dissolution in the initial stage:

$$dC/dt = K_1 \{ C_{SA} \exp(-K_r t) + C_{SH} [1 - \exp(-K_r t)] \} \quad (1)$$

$$C = K_1 (C_{SA} - C_{SH}) [1 - \exp(-K_r t)] / K_r + K_1 C_{SH} t \quad (2)$$

where C is the concentration of the drug in bulk solution, C_{SA} and C_{SH} are the solubilities of the anhydrate and hydrate, respectively, t is time, K_1 is the dissolution rate constant and K_r is the rate constant of the phase transformation process.

Since it can be assumed that the diffusion constant of the amorphous form is the same as that of form C, the data were analyzed by Eq. 2, and the kinetic parameters in Eq. 1 were estimated. C_s was measured by the dispersed-amount method and K_1 was calculated from the initial dissolution rate of the hydrate, respectively. K_r and C_{sm} of piretanide were estimated using the nonlinear least-squares computer program MULTI.¹²⁾ However, we did not use the initial dissolution data of the amorphous form in the early stage at 45 °C for this calculation of K_r , because the amorphous form was changed faster than at other temperatures (30–40 °C).

These parameters (K_r and C_{sm}) are $1.30 \times 10^{-1} \text{ min}^{-1}$ and 449.6 mg/100 ml at 30 °C, $4.55 \times 10^{-1} \text{ min}^{-1}$ and 464.0 mg/100 ml at 35 °C and $8.15 \times 10^{-1} \text{ min}^{-1}$ and 521.0 mg/100 ml at 40 °C, respectively, given in Table 2. The theoretical values (shown by the solid lines in Fig. 5) were in good agreement with the observed values under all dissolution conditions. The kinetic parameters es-

Table 2. Saturated Concentrations (C_{sm} and C_{so}) and Rate Constants of Crystallization and Dissolution (K_r and K_1) at Various Temperatures with Stirring at 200 rpm

Temperature (°C)	C_{sm} (mg/100 ml)	C_{so} (mg/100 ml)	$K_r \times 10^{-1}$ (min ⁻¹)	$K_1 \times 10^{-4}$ (min ⁻¹)
30	449.6	33.7	1.30	3.30
35	464.0	40.8	4.55	4.12
40	521.0	51.4	8.15	4.35

$n=3$.

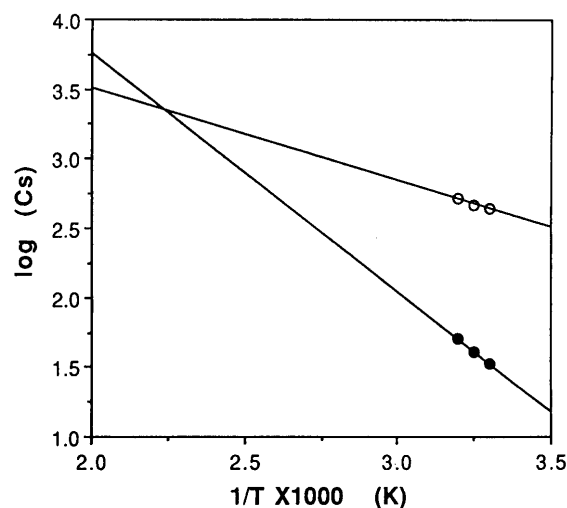


Fig. 6. Van't Hoff Plots for Piretanide Amorphous Form and Form C at pH 5

○, amorphous form; ●, form C.

Table 3. Thermodynamic Parameters of the Amorphous Form and Form C at pH 5

Sample	Transition temperature (°C)	Heat of solution (kJ/mol)	Heat of transition (kJ/mol)
Amorphous form		12.7	
Form C	174	32.8	-20.1

$n=3$.

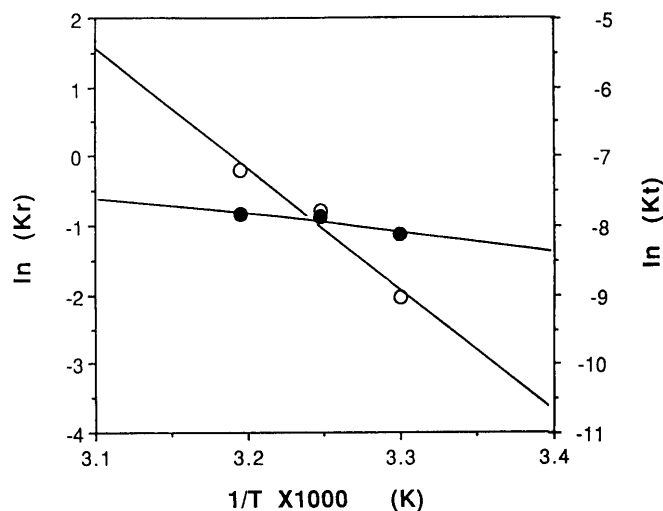


Fig. 7. Arrhenius Plots of Phase Transformation and Dissolution Process at pH 5

○, transformation process; ●, dissolution process.

Table 4. Activation Energies (E) for Phase Transition and the Dissolution Process

Sample	E (kJ/mol)	
	Phase transformation	Dissolution
Piretanide amorphous form ($n=3$)	145.5	21.7
<i>p</i> -Hydroxybenzoic acid anhydrate	59.0	14.6
Phenobarbital anhydrate	41.8	15.2
Chlorpropamide anhydrate	57.4	16.3
Nitrofurantoin anhydrate	22.1	12.4

timated by a nonlinear curve-fitting program are summarized in Table 2.

Figure 6 shows the van't Hoff plot for the saturated concentration of the amorphous form and form C. These plots showed a linear relationship within the temperature range studied and the intersection of the extension of the two straight lines is at about 174 °C. The heat of the solution (Table 3) was estimated from the slope of the line.

Figure 7 shows an Arrhenius plot for phase transformation and the dissolution processes of the amorphous form. The activation energies for both processes calculated from the slopes of the regression lines are summarized in Table 4. The activation energy for the dissolution process of piretanide amorphous form was 1.3–1.8 times larger than that reported for the dissolution process involving a phase change,^{2,5,8)} and the value for the phase transformation process was 5–7 times larger than the reported data for organic medicines.^{2,5,8)} This result also supports the view that polymorphs transform during the initial

dissolution stage.

Conclusion

In this study, amorphous form and form C were about 4.5-fold more soluble than the stable form A and the metastable form B in JP XII second fluid (pH 6.8). Despite being metastable, form C was stable without polymorphic transformation at various pH. However, the amorphous form was polymorphically transformed into form C at various pH. These results suggested that the amorphous form and form C would be more bioavailable than forms A and B.

References

- 1) Chikaraishi Y., Otsuka M., Matsuda Y., *Chem. Pharm. Bull.*, **43**, 1966–1969 (1995).
- 2) Ueda H., Nambu N., Nagai T., *Chem. Pharm. Bull.*, **32**, 244–250 (1984).
- 3) Shefter E., Higuchi T., *J. Pharm. Sci.*, **52**, 781–791 (1963).
- 4) Wurster D. E., Taylor P. W., Jr., *J. Pharm. Sci.*, **54**, 670–676 (1965).
- 5) Nogami H., Nagai T., Yotsuyanagi T., *Chem. Pharm. Bull.*, **17**, 499–509 (1969).
- 6) Kaneniwa N., Ichikawa J., Matsumoto T., *Chem. Pharm. Bull.*, **36**, 1063–1073 (1988).
- 7) Otsuka M., Teraoka R., Matsuda Y., *Chem. Pharm. Bull.*, **39**, 2667–2670 (1991).
- 8) Otsuka M., Teraoka R., Matsuda Y., *Pharmaceutical Research*, **9**, 307–311 (1992).
- 9) Chikaraishi Y., Otsuka M., Matsuda Y., *Chem. Pharm. Bull.*, **44**, 1614–1617 (1996).
- 10) Clark W. M., Lubs H. A., *J. Bact.*, **2**, 1–34, 109–136, 191–236 (1917).
- 11) Miller G. L., Golder R. H., *Arch. Biochem.*, **29**, 420–423 (1950).
- 12) Yamaoka T., Tanigawara T., Nakagawa T., Uno T., *J. Pharmacobiodyn.*, **4**, 879–885 (1981).